

## In silico identification and biochemical characterization of novel inhibitors of NQO1

Karen A. Nolan,<sup>a</sup> David J. Timson,<sup>b</sup> Ian J. Stratford<sup>a,\*</sup> and Richard A. Bryce<sup>a,\*</sup>

<sup>a</sup>*School of Pharmacy and Pharmaceutical Sciences, University of Manchester, Oxford Road Manchester M13 9PL, UK*

<sup>b</sup>*School of Biological Sciences, Queen's University Belfast, Medical Biology Centre, 97 Lisburn Road, Belfast BT9 7BL, UK*

Received 7 August 2006; revised 4 September 2006; accepted 7 September 2006

Available online 29 September 2006

**Abstract**—From in silico docking and COMPARE analysis, novel inhibitors of human NAD(P)H quinone oxidoreductase (NQO1) have been identified from the NCI compound database, the most potent of which has an observed IC<sub>50</sub> of 0.7  $\mu$ M. The inhibitors exhibit a diverse range of scaffolds. The ability of docking calculations to predict experimentally determined binding affinities for NQO1 is discussed, considering the influence of target flexibility and scoring function.

© 2006 Elsevier Ltd. All rights reserved.

Human NAD(P)H quinone oxidoreductase (NQO1, DT diaphorase, EC 1.6.99.2) is a homodimeric enzyme with one molecule of non-covalently bound FAD per monomer.<sup>1</sup> It is biochemically characterized by its unique ability to use either NADH or NADPH as reducing cofactors with equal efficiency.<sup>2</sup> NQO1 is widely distributed in animals, plants, and bacteria. In humans, it is constitutively expressed in a variety of tissues throughout the body with highest levels in epithelial and endothelial cells, particularly of the kidney and gastrointestinal tract.<sup>3</sup> NQO1 is over-expressed in many solid tumours compared to surrounding normal tissue, thus making it an attractive target for selective anti-cancer drug development.<sup>4</sup> The enzyme is an oxygen independent two electron reductase that functions as a protective enzyme,<sup>5</sup> an antioxidant enzyme,<sup>6</sup> and an enzyme capable of bioactivating a variety of prodrugs, such as EO9 and RH1, to their cytotoxic species (Fig. 1).<sup>7</sup>

The catalytic mechanism of action of NQO1 relies on sequential two electron transfer from NAD(P)H to FAD to the substrate.<sup>1</sup> This so-called ‘ping-pong’ reaction is competitively inhibited by the anticoagulant dicoumarol (Fig. 1).<sup>8</sup> Additionally, the mechanism-based suicide inhibitor ES936 has been shown to bind and alkylate the active site of the enzyme (Fig. 1).<sup>9</sup> Recent

evidence suggests another role of NQO1 may be to defend cells against oxidative damage. This is supported by both dicoumarol and ES936 being able to inhibit the growth of high NQO1 expressing pancreatic tumour cells in vitro and in vivo.<sup>10</sup>

Several crystal structures of NQO1 have been solved making a structure-based drug discovery approach possible. The crystal structures of NQO1 show that two domains form each monomer: an N-terminal catalytic domain (residues 1–221) and a C-terminal domain (residues 222–274) which is involved in dimerization.<sup>11</sup> The catalytic domain comprises a central parallel  $\beta$ -sheet in the middle of a number of connecting helices whilst the smaller C-terminal domain is composed of an anti-parallel hairpin motif, an  $\alpha$ -helix and several loops.<sup>1,11</sup> Two independent active sites are located at opposite ends of the dimer and contain residues from each monomer. The active sites are essentially large hydrophobic pockets where the NAD(P)H cofactor and substrate can bind independently. The active site of NQO1 can accommodate a broad range of substrates.<sup>1,12</sup>

In the present study, we applied a virtual screening approach to identify potential candidate ligands for NQO1 (either novel substrates or inhibitors for lead optimization). This strategy involved a hierarchical computational screening of the National Cancer Institute (NCI) database using computational molecular docking. The database was selected on the basis that biological data were available for many of the compounds. The NCI inventory contains over 700,000

**Keywords:** NQO1; Inhibitors; Rational drug design; Virtual screening; Docking; Scoring functions.

\* Corresponding authors. E-mail: [r.a.bryce@manchester.ac.uk](mailto:r.a.bryce@manchester.ac.uk)

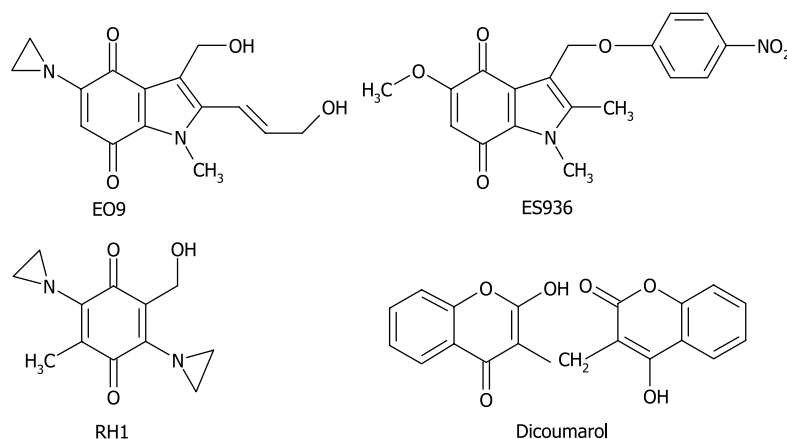


Figure 1. Known substrates and inhibitors of NQO1.

contributed compounds and includes both natural and synthetic structures (<http://www.dtp.nih.gov>).<sup>13</sup> Additionally, the NCI conducts an anti-cancer drug development programme which provides an initial in vitro screen to evaluate compounds for potential anti-cancer activity. The NCI in vitro cancer screen is unique since the results of any compound showing promise are used to produce a biological response pattern which is then utilized in pattern recognition algorithms such as COMPARE.<sup>13</sup> The COMPARE algorithm may be used to determine a potential mechanism of action of a test compound or identify whether the biological response pattern is similar to any other compounds included in the NCI database.<sup>14</sup> Furthermore, following characterization of various molecular targets in the 60 cell line panel, it may be feasible to select compounds most likely to interact with a specific molecular target.<sup>14</sup> Here, we applied both database searching methods, with subsequent biochemical evaluation for their ability to act as substrates or inhibitors of NQO1.

Docking calculations initially used DOCK 4.0,<sup>15</sup> based on its previous performance in our hands<sup>16</sup> and others.<sup>17</sup> Docking was conducted using the crystal structure of human NQO1 with the co-crystallized ligand EO9 removed (PDB entry 1GG5; 2.5 Å).<sup>12</sup> The active site of human NQO1, based around residues Trp105, Phe106, Gly149, Gly150, Tyr155, His161, His194, Pro68', Tyr126', Tyr128', Gly174', Phe178', and FAD (Fig. 2), was used to generate a Connolly molecular surface with a probe radius of 1.4 Å. A 58 sphere negative image of the active site was generated. A scoring grid (resolution of 0.3 Å/grid point) was calculated based on the AMBER united atom forcefield and charges. A distance-dependent dielectric function of  $4.0r$ , a non-bonded energy cutoff distance of 10 Å and a bump overlap of 0.75 Å was used. Ligands were assigned Gasteiger–Marsili charges<sup>18</sup> and 3-D coordinates using the program CORINA.<sup>19</sup> These compounds are referred to by their unique NSC identifier using the NCI convention. SYBYL 6.8 was used for molecular visualization.<sup>20</sup>

Prior to docking of the NCI database, a series of validation tests were performed to ascertain the optimal

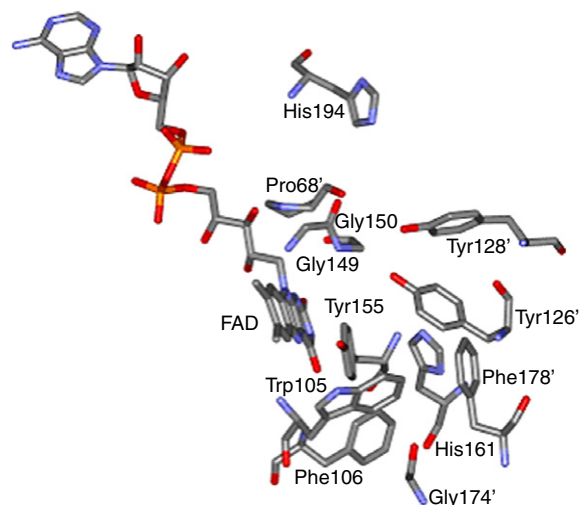


Figure 2. The active site residues of human NQO1.

computational parameters for docking via DOCK. The quality of docking was assessed by comparing the root mean square deviation (RMSD) of the docked pose to that of the crystal structure. EO9 was docked back into the active site of NQO1 with an RMSD of 1.3 Å from the crystal structure (the quinone ring was <0.9 Å). The in silico screening strategy involved an initial filter to select for bioavailability using in-house software.<sup>16</sup> This removed ligands of greater than 500 g/mol and absolute charge of greater than  $1e$ .<sup>21</sup> The NCI database was then subject to rigid-body docking from which the top-ranked 2000 compounds were retained for further analysis via flexible ligand docking. The top 200 highest scoring compounds were further filtered by identifying appealing interactions and by pharmacokinetic considerations.<sup>21</sup> Of the 100 top-ranked compounds, 21 were available for biochemical evaluation from the NCI repository.

The COMPARE database was also mined using NQO1 as a molecular target to identify compounds that statistically may be potential substrates or inhibitors.<sup>13</sup> All hits were then docked allowing full ligand flexibility to ascertain binding mode and affinity. Of the 25

compounds requested from the NCI repository, 7 compounds were available for assay.

The combined set of 28 compounds from the two database searches was evaluated for biological activity as follows: recombinant human NQO1 was prepared and purified as described by Phillips.<sup>22</sup> The enzyme was then diluted in 50 mM phosphate buffer to give an absorbance of 0.1 at 550 nm; 5  $\mu$ l of this solution was then mixed with 495  $\mu$ l of 50 mM phosphate buffer containing 200  $\mu$ M NADH, 70  $\mu$ M cytochrome c, 2  $\mu$ M BSA, various concentrations of the potential inhibitor dissolved in DMSO (maximum concentration 0.5% v/v) and 3  $\mu$ M menadione at pH 7.4. This concentration of menadione was chosen to correspond to the  $K_m$  value for this substrate determined under the same conditions. The DMSO concentration used is sufficiently small to ensure minimal perturbation of hydrogen bonding networks in aqueous NQO1 complexes. Reactions were carried out at 25 °C and cytochrome c reduction was monitored at 550 nm in a Beckman DU 650 spectrophotometer.  $IC_{50}$  values were determined using nonlinear curve fitting as implemented in the program Excel for which a 50% reduction of the initial rate was attained. Each compound was also tested for its ability to act as a substrate by repeating the experiment in the absence of menadione. All reactions were carried out in triplicate and all of the compounds evaluated transpired to be inhibitors. The 28 compounds are ranked according to  $IC_{50}$  in Table 1.

Calculated binding energies from DOCK for the 200 top-ranked ligands ranged up to –61 kcal/mol and were significantly higher than for the crystallographic ligand EO9 (–39 kcal/mol) or for the competitive inhibitor, dicoumarol (–38 kcal/mol). The docking studies confirm that the active site of NQO1 can accommodate ligands of different size and structure, adopting a variety of binding modes and interactions. This is demonstrated by the number of structurally diverse scaffolds shown in Table 1. Most ligands made at least two hydrogen bond contacts with active site residues, primarily Tyr126', Tyr128', and His161 (Fig. 2); these residues are known to be important in the catalytic mechanism of NQO1.<sup>1</sup> Furthermore, many of the compounds made additional hydrogen bonds with other residues such as Gly149, Gly150, and His194 (Fig. 2). However, this was largely seen with the higher molecular weight molecules. Compounds with heteroaromatic ring systems appeared to stack between the FAD and Phe178' via  $\pi$ -overlap with the isoalloxazine ring. Further hydrophobic interactions were made with Trp105 and Phe106. Eight out of the top 100 ranked compounds from the *in silico* screen possessed an acridine-based motif, perhaps not unexpected given the planar nature of these intercalators.

Interestingly, the compound ranked 23rd out of 200 from the *in silico* screen with a binding energy of –51 kcal/mol was AQ4M (NSC684664, Fig. 3 and Table 1), the mono *N*-oxide anthraquinone intermediate in the metabolism of bioreductive drug AQ4N which is currently in Phase I/II clinical trials. The calculated binding of the prodrug AQ4N and its putative cytotoxic product

AQ4 were consequently assessed and also demonstrated strong affinity for NQO1 (–54 and –52 kcal/mol, respectively). Although dicoumarol showed a relatively low calculated binding energy, it remained the most efficient competitive inhibitor of NQO1-mediated reduction of menadione ( $IC_{50}$  = 0.45  $\mu$ M).

No clear correlation could be established between the calculated binding affinity and experimentally determined  $IC_{50}$  values for the 28 ligands. In a bid to improve the correlation between  $IC_{50}$  and calculated score, the ligand set was re-evaluated using the two scoring functions GoldScore and ChemScore, implemented in the genetic algorithm-based docking program, GOLD2.2.<sup>23</sup> The GOLD method allows a limited degree of side-chain flexibility (terminal H rotations). A validation test was performed using GOLD/ChemScore, where EO9 was docked back into its crystal structure with an RMSD of 0.6 Å (see Supplementary Data). However, for the 28 compounds, once again no significant correlation with  $IC_{50}$  could be ascertained with either GoldScore or ChemScore scoring functions. We did observe a weak relationship ( $r^2$  = 0.5) between DOCK and ChemScore energies (Table 1).

In an effort to include more protein flexibility in docking calculations, two further crystal structures of human NQO1 were studied: PDB entry 1KBQ (1.8 Å),<sup>24</sup> a complex with mechanism-based inhibitor ES936; and PDB entry 1H66 (2.0 Å)<sup>12</sup>, containing the bioreductive drug RH1 (Fig. 1). The differences in active site conformation have been described previously and reflect modest changes in the side-chain conformations of Tyr126', Tyr128', and mainly His161.<sup>25</sup> For validation, all three crystal ligands were docked back into their native complexes using DOCK or GOLD/ChemScore: an RMSD of <1.4 Å was found, and all native hydrogen bonds were recovered.

For the set of 28 compounds, the binding modes for many of the docked poses from DOCK and GOLD/ChemScore were positioned in a similar spatial orientation in the active site and made comparable binding interactions; this was true across the three protein crystal structures. The compound with the best measured  $IC_{50}$ , NSC645827 (Table 1), stacks against the isoalloxazine ring in the active site of human NQO1, forming polar contacts with Tyr126', Tyr128', Gly150, and His161 (Fig. 4). Compound NSC645808, which differs from NSC645827 in the substitution of a N atom with a C atom in the five-membered heteroaromatic ring (Table 1), lacks a polar contact with His161 and thus may contribute to its 14-fold reduced inhibitory activity relative to NSC645827. DOCK and ChemScore rankings were found not to vary significantly across the three crystal structures (cross-correlation of  $r^2$  > 0.8 for all combinations, Supplementary Data). Consequently, no improvement in correlation between the calculated binding energies and the biochemical data by using the three crystal geometries was obtained, reflecting the modest difference in active site conformation across the three crystal structures.<sup>25</sup>

**Table 1.** 28 NCI compounds, their chemical structure, experimental IC<sub>50</sub> values and DOCK interaction energy (kcal/mol)

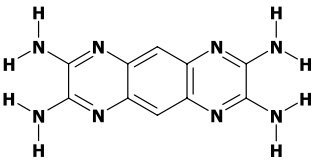
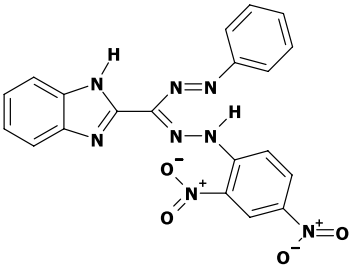
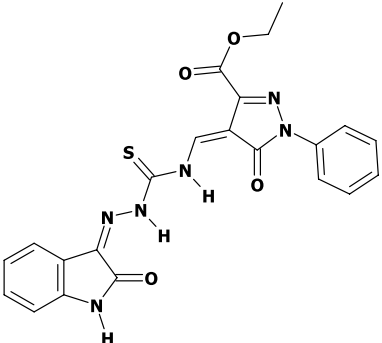
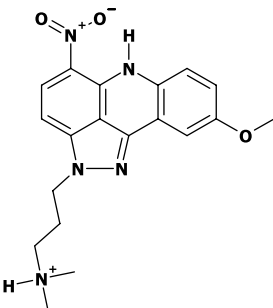
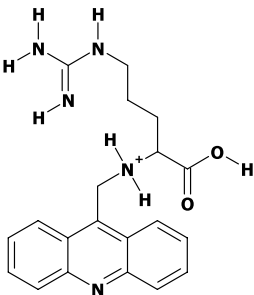
NSC	Heavy atoms	Chemical structure	$U_{\text{bind}}^a$	IC <sub>50</sub> (μM)
645827	24		−49.9 (−31.9)	0.7
339583	28		−53.4 (−29.6)	2
354279	25		−51.5 (34.21)	2
275420	24		−51.3 (−37.9)	3
339580	29		−59.1 (−26.0)	3
2113 <sup>b</sup>	12		−27.6 (−27.4)	3.5
73410	24		−52.6 (−26.1)	7.5
106547 <sup>b</sup>	18		−36.8 (−38.7)	10

(continued on next page)

Table 1 (continued)

NSC	Heavy atoms	Chemical structure	$U_{\text{bind}}^{\text{a}}$	$\text{IC}_{50}$ ( $\mu\text{M}$ )
645808	24		−52.4 (−32.9)	10
224124	24		−51.3 (−33.5)	12.5
316158	26		−53.7 (−28.6)	17.5
8735 <sup>b</sup>	9		−20.5 (−24.5)	20
25415 <sup>b</sup>	14		−30.6 (−27.0)	22.5
337766	30		−58.3 (−37.6)	25
600586	28		−55.3 (−39.5)	25

Table 1 (continued)

NSC	Heavy atoms	Chemical structure	$U_{\text{bind}}^a$	IC <sub>50</sub> (μM)
667757	18		−31.9 (−18.3)	25
353671	32		−48.7 (−37.5)	35
659692	33		−52.3 (−28.5)	35
627168	27		−52.4 (−34.6)	45
627736	27		−50.0 (−35.2)	45

(continued on next page)

Table 1 (continued)

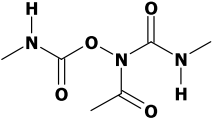
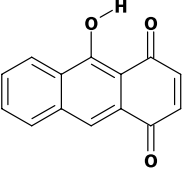
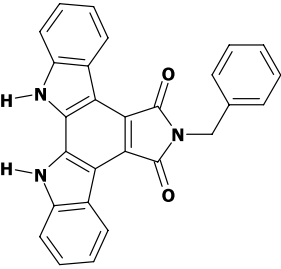
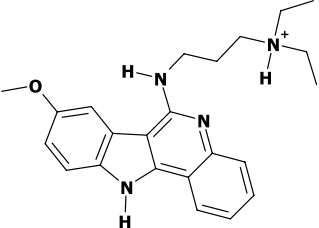
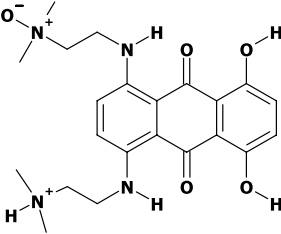
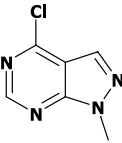
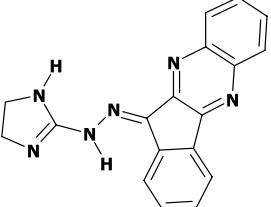
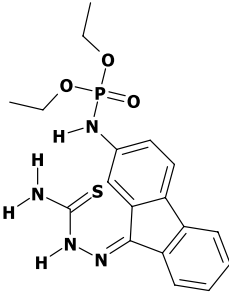
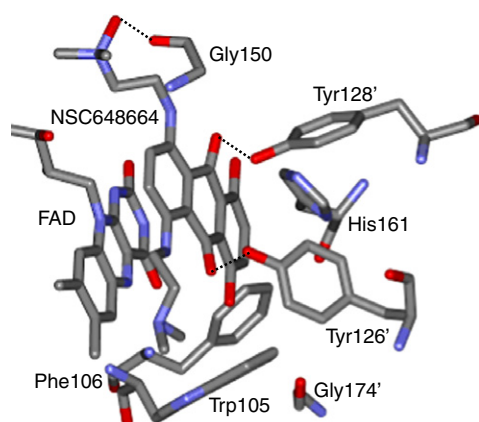
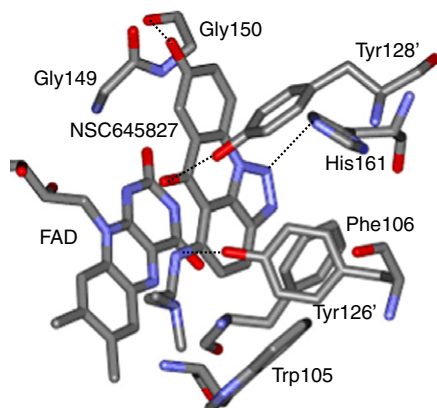
NSC	Heavy atoms	Chemical structure	$U_{\text{bind}}^{\text{a}}$	$\text{IC}_{50}$ ( $\mu\text{M}$ )
253272 <sup>b</sup>	13		−26.2 (−14.2)	55
618201 <sup>b</sup>	17		−36.1 (−30.5)	60
628440	32		−53.4 (−39.1)	90
664238	28		−53.3 (−42.7)	90
684664	31		−51.4 (−28.4)	95
1424 <sup>b</sup>	11		−23.9 (−18.3)	105
658835	24		−51.7 (−42.4)	150

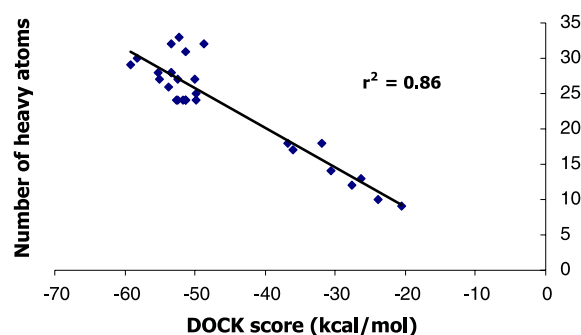


Table 1 (continued)

NSC	Heavy atoms	Chemical structure	$U_{\text{bind}}^a$	IC <sub>50</sub> (μM)
102359	27		−55.1 (−30.8)	250

<sup>a</sup> ChemScore binding energy values (kcal/mol) in parentheses.<sup>b</sup> Signifies compounds identified from the COMPARE screen.**Figure 3.** NSC648664 in the active site of NQO1. Polar contacts are shown as dashed lines.**Figure 4.** NSC645827 in the active site of NQO1. Polar contacts are shown as dashed lines.

Although no relationship could be established between calculated binding affinity and experimentally determined IC<sub>50</sub> values, despite including target flexibility and exploring different scoring functions, a clear correlation exists between the number of heavy atoms and the calculated energy score ( $r^2 = 0.86$ , Fig. 5). This is interesting since Kuntz et al.<sup>26</sup> demonstrated that the experimental free energy of binding for a wide range of ligands to a variety of macromolecular targets

**Figure 5.** Number of heavy atoms versus DOCK energy score for compounds in Table 1.

increased with the number of ligand non-hydrogen atoms. However, for ligands containing more than 15 non-hydrogen atoms, the free energy of binding increased very little with relative molecular mass (attributed to non-thermodynamic factors).<sup>26</sup> A subsequent analysis of the dominant interactions of the ligands studied by Kuntz et al. suggested that van der Waals contacts and hydrophobic effects may provide a rationale for understanding binding affinities across a diverse set of ligands.<sup>26</sup> Whereas the DOCK energy function behaves according to this observed relationship (Fig. 5), the experimental IC<sub>50</sub> data here interestingly do not, although one might expect such a hypothesis to be particularly pertinent to ligands binding into the largely hydrophobic active site of NQO1.

In conclusion, using both in silico docking and COMPARE analysis, novel inhibitors of human NQO1 have been identified from the NCI compound database, exhibiting a diverse range of scaffolds including, for example, acridine-based frameworks. Although lower affinity than the known competitive inhibitor, dicoumarol (IC<sub>50</sub> = 0.45 μM), the most potent inhibitor identified here, NSC645827 (IC<sub>50</sub> = 0.7 μM), satisfies all the criteria proposed by Lipinski for a ligand with favourable pharmacokinetic properties for future optimization.<sup>21</sup> These compounds were identified despite difficulty in demonstrating a significant relationship between calculated and experimental binding affinity, even including target flexibility and exploring different



scoring functions.<sup>27</sup> A relationship was found between calculated binding energy and the number of non-hydrogen ligand atoms, reflecting the steric complementarity and hydrophobicity of the active site of NQO1, and mirroring a previous empirically observed correlation.

### Acknowledgments

The authors gratefully acknowledge a MRC Chemical Biology Ph.D. studentship (K.A.N.) and a MRC programme grant (I.J.S.).

### Supplementary data

Supplementary data associated with this article can be found, in the online version, at [doi:10.1016/j.bmcl.2006.09.015](https://doi.org/10.1016/j.bmcl.2006.09.015).

### References and notes

- Li, R.; Bianchet, M. A.; Talay, P.; Amzel, L. M. *Proc. Natl. Acad. Sci. U.S.A.* **1995**, *92*, 8846.
- Lind, C.; Cadenas, E.; Hochstein, P.; Ernster, L. *Methods Enzymol.* **1990**, *186*, 287.
- Jaiswal, A. K.; McBride, O. W.; Adesnik, M.; Nebert, D. W. *J. Biol. Chem.* **1988**, *263*, 13572.
- Schlager, J.; Powis, G. *Int. J. Cancer* **1990**, *45*, 403.
- Smith, M. T. *Proc. Natl. Acad. Sci. U.S.A.* **1999**, *96*, 7624.
- Seigel, D.; Gustafson, D. L.; Dehn, D. L.; Han, J. Y.; Boonchoong, P.; Berliner, L. J.; Ross, D. *Mol. Pharm.* **2004**, *65*, 1238.
- Begleiter, A.; Leith, M. K.; Curphrey, T. J.; Doherty, G. P. *Oncol. Res.* **1997**, *9*, 371.
- Ernster, L. *Methods Enzymol.* **1967**, *10*, 309.
- Dehn, D. L.; Siegel, D.; Swann, E.; Moody, C. J.; Ross, D. *Mol. Pharm.* **2003**, *64*, 714.
- Cullen, J. J.; Hinkhouse, M. M.; Grady, M.; Gaut, A. W.; Liu, J. R.; Zhang, Y. P.; Weydert, C. J. D.; Domann, F. E.; Oberley, L. W. *Cancer Res.* **2003**, *63*, 5513.
- Faig, M.; Bianchet, M. A.; Talalay, P.; Chen, S.; Winski, S.; Ross, D.; Amzel, L. M. *Proc. Natl. Acad. Sci. U.S.A.* **2000**, *97*, 3177.
- Faig, M.; Bianchet, M. A.; Winski, S.; Hargreaves, R.; Moody, C. J.; Hudnott, A. R.; Ross, D.; Amzel, L. M. *Structure* **2001**, *9*, 659.
- Fitzsimmons, S. A.; Workman, P.; Grever, M.; Paull, K.; Camalier, R.; Lewis, A. D. *J. Natl. Cancer Inst.* **1996**, *8*, 259.
- Tudor, G.; Gutierrez, P.; Aguilera-Gutierrez, A.; Sausville, E. A. *Biochem. Pharm.* **2003**, *65*, 1061.
- Ewing, T. J. A.; Makino, S.; Skillman, A. G.; Kuntz, I. D. *J. Comput. Aided Mol. Des.* **2001**, *15*, 411.
- McNally, V. A.; Gbaj, A.; Douglas, K. T.; Stratford, I. J.; Jaffar, M.; Freeman, S.; Bryce, R. A. *Bioorg. Med. Chem. Lett.* **2003**, *13*, 3705.
- Aronov, A. M.; Munagala, N. R.; de Montellano, P. R. O.; Kuntz, I. D.; Wang, C. C. *Biochemistry* **2000**, *39*, 4684.
- Gasteiger, J.; Marsili, M. *Tetrahedron* **1980**, *36*, 3219.
- Gasteiger, J.; Rudolf, C.; Sadowski, J. *Tetrahedron* **1990**, *3*, 537.
- SYBYL 6.8; Tripos Inc.: St Louis, MO, USA **2003**.
- Lipinski, C. A.; Lombardo, F.; Dominy, B. W.; Feeney, P. J. *Adv. Drug Deliv. Rev.* **1997**, *23*, 3.
- Phillips, R. M. *Biochem. Pharmacol.* **1999**, *58*, 303.
- Jones, G.; Willett, P.; Glen, R. C.; Leach, A. R.; Taylor, R. J. *Mol. Biol.* **1997**, *267*, 727.
- Winski, S. L.; Faig, M.; Bianchet, M. A.; Siegel, D.; Swann, E.; Fung, K.; Duncan, M. W.; Moody, C. J.; Amzel, M.; Ross, D. *Biochemistry* **2001**, *40*, 15135.
- Bianchet, M. A.; Faig, M.; Amzel, L. M. *Methods Enzymol.* **2004**, *382*, 144.
- Kuntz, I. D.; Chen, K.; Sharp, K. A.; Kollman, P. A. *Proc. Natl. Acad. Sci. U.S.A.* **1999**, *96*, 9997.
- Blaney, J. M.; Dixon, J. S. *Perspect. Drug Discovery Des.* **1993**, *1*, 301.